

45th Aerospace Sciences Meeting and Exhibit
8-11 January 2006 / Reno, NV

AIAA-2007-1387

Methanol and Ethanol Ignition by Repetitively Pulsed, Nanosecond Pulse Duration Plasma¹

Ainan Bao², Yurii G. Utkin³, Saurabh Keshav², and Igor V. Adamovich⁴

*Nonequilibrium Thermodynamics Laboratories, Department of Mechanical Engineering
The Ohio State University, Columbus, OH 43210*

Abstract

The paper presents results of plasma assisted ignition of liquid hydrocarbon fuel flows excited by a low-temperature, transverse, repetitively pulsed discharge plasma. The experiments have been conducted with methanol and ethanol fuels injected into a flow of dry air, at pressures of $P=70-90$ torr and flow velocities of $u=13-32$ m/sec. Experiments showed that preheating of the air fuel up to $50-60^{\circ}$ C is essential for accelerating fuel evaporation in the test section. On the other hand, fuel preheating does not significantly affect fuel evaporation rate. Uniform and diffuse nonequilibrium plasma in the test section was generated by high-voltage (16-18 kV), short pulse duration (20-30 nsec), high repetition rate ($\nu=50$ kHz) pulses. In ethanol-air flows at $P=70$ torr, $u=16$ m/sec, $\Phi=0.8-1.2$, and $T_{\text{air}}=T_{\text{fuel}}=60^{\circ}$ C, ignition was achieved but combustion was unstable, due to inadequate fuel injector operation (poor spray pattern) at low fuel delivery pressures and mass flow rates, $\dot{m}_{\text{fuel}}=0.08-0.12$ g/sec. In a methanol-air flow at the baseline conditions, at $P=90$ torr, $u=13$ m/sec, $\Phi=1.2$, and $T_{\text{air}}=T_{\text{fuel}}=60^{\circ}$ C ($\dot{m}_{\text{fuel}}=0.16$ g/sec), ignition was achieved and stable combustion was maintained. At these conditions, the plasma temperatures before and after fuel injection were $T=240^{\circ}$ C and $T=480^{\circ}$ C, respectively, and a significant fraction of injected fuel reacted, up to 75%. Both increasing the flow velocity, up to $u=26$ m/sec, and reducing the air flow temperature, down to $T_{\text{air}}=20^{\circ}$ C, resulted in drastic reduction of reacted fuel fraction, to just a few per cent. On the other hand, decreasing the fuel preheating temperature, down to $T_{\text{fuel}}=20^{\circ}$ C, did not result in a significant change of the amount of reacted fuel, which remained in the range of 30-60%. Temperature rise in the plasma caused by fuel injection is proportional to the amount of fuel vapor present in the flow without the plasma. The experiments suggest that preheating the air flow is critical for ignition, while fuel preheating may not be necessary.

¹ Copyright ©, American Institute of Aeronautics and Astronautics. All rights reserved

² Graduate Research Assistant

³ Post-Doctoral Researcher

⁴ Associate Professor, Associate Fellow AIAA

1. Introduction

Over the last few years, considerable progress has been made in studies of ignition and flame stabilization by low-temperature nonequilibrium plasmas (e.g. see recent reviews [1,2] and references therein). In particular, recent experiments on ignition of premixed hydrocarbon-air flows using transverse RF discharge plasma and nanosecond duration repetitively pulsed plasma demonstrated that large-volume ignition can be produced at plasma temperatures significantly lower than the autoignition temperature, by at least 300-400⁰ C [3-6]. These experiments also showed that low-temperature plasma ignition and flameholding can be achieved at significantly lower pressures and higher flow velocities compared to capacitor spark and DC arc ignition [3], in a wide range of equivalence ratios and at a relatively modest plasma power budget (a few per cent of the fuel heating value) [4-6]. Experiments on ignition of non-flowing preheated hydrogen-air and hydrocarbon-air mixtures by a single-pulse fast ionization wave discharge [7,8] demonstrated that ignition delay time can be substantially reduced compared to autoignition at the same temperature. Finally, repetitively pulsed nanosecond duration plasma has been shown to stabilize lean premixed atmospheric pressure propane-air flames, increase the flame blow-off velocity, and expand the flammability limits, at a very small plasma power budget (~0.1% of the burner power) [9-12]. The results also suggest that chemically active species generated in the plasma, such as oxygen atoms and OH radical, may play critical role in kinetics of low-temperature plasma fuel oxidation and ignition [10,13,14].

These recent advances suggest a possibility of developing an energy-efficient nonequilibrium plasma ignition and flame stabilization method, which could be used both at low pressures and high flow velocities, as well as in fuel lean mixtures, i.e. when common ignition approaches are ineffective. In particular, our recent work demonstrated the use of high-voltage, short pulse duration, high pulse repetition rate discharge for this purpose. This discharge offers two critical advantages over DC, AC, RF, and microwave discharge plasmas. First, the short pulse duration in this type of discharge greatly improves the plasma stability. Basically, the pulse duration, a few tens of nanoseconds, is much shorter than the characteristic time for the ionization instability development and glow-to-arc transition $\sim 10^{-3}$ - 10^{-4} sec [15]. This makes possible operating this discharge at much higher pressures and power loadings compared to other types of nonequilibrium plasmas. Also, the reduced electric field, E/N, during the high voltage pulses results in efficient ionization, electronic excitation, and dissociation of molecular species by electron impact, the rates of which have strong exponential dependence on E/N [15]. This may result in generation of large amounts of active radical species at a relatively low plasma power budget. Previously, this type of discharge has been successfully used by our group for sustaining high levels of ionization in high-speed, low-temperature MHD flow control experiments [16,17] and singlet oxygen generation in high-pressure discharges [18,19].

The objective of the present work is to expand the range of applicability of the repetitively pulsed nanosecond duration discharge, and to study feasibility of ignition of liquid hydrocarbon fuels injected in the air flow using this approach.

2. Experimental

The experiments have been conducted at the OSU high-speed flow plasma combustion facility [3-7]. The schematic of the facility is shown in Fig. 1. Air flow enters the 5 cm x 1 cm

rectangular cross section, 31 cm long test section through a 1 inch diameter gas supply line. The facility can use either room air or cylinder air. The air mass flow rate is determined by measuring pressure upstream of a sonic choke plate (insert with a pinhole of known area) placed in the air delivery line. The air flow can be preheated up to $T=200^{\circ}\text{C}$ using a 6 kW in-line flow heater placed upstream the test section (see Fig. 1). When the heater is used, the flow temperature in the test section (in the absence of the plasma) is monitored by a thermocouple inserted through a port in the top of the test section, as shown in Fig. 2.

Downstream of the heater and approximately 30 cm upstream of the test section, liquid fuel (methanol or ethanol) is injected into the air delivery line from an M1 fine atomizing spray nozzle (Danfoss Hago Inc.). The nozzle is rated to produce $40\ \mu\text{m}$ to $17\ \mu\text{m}$ diameter droplets into a full cone spray angle of 80° within the flow rate range of $0.66\ \text{cm}^3/\text{sec}$ to $2.35\ \text{cm}^3/\text{sec}$ ($\dot{m}_{\text{fuel}}=0.52\text{-}1.85\ \text{g}/\text{sec}$). However, at the present conditions the mass flow rate of fuel was typically considerably lower, $\dot{m}_{\text{fuel}}=0.1\text{-}0.2\ \text{g}/\text{sec}$, which adversely affected the fuel spray pattern. The fuel is delivered from a stainless steel bubbler pressurized by compressed air up to $P=80\ \text{psi}$, shown in Fig. 1. The flow rate of the fuel, which can also be preheated using a tape heater wrapped around a $1/4$ " inch diameter copper delivery line, is monitored by a flow meter. The fuel temperature is measured by a thermocouple placed between the copper tube and the heater. In the present experiments, both the air and the fuel flows were preheated to $T=20\text{-}60^{\circ}\text{C}$. Preheating was used to accelerate the rate of fuel evaporation in the air flow and to prevent excessive cooling of the air-fuel mixture during evaporation. The saturated vapor pressures of methanol and ethanol at $T=20^{\circ}\text{C}$ are 92 torr and 45 torr, respectively, which implies complete fuel evaporation at thermodynamic equilibrium at the present conditions. However, complete evaporation of ethanol in a stoichiometric liquid ethanol / air mixture (6.5% $\text{C}_2\text{H}_5\text{OH}$ by volume) would result in its cooling by about 80°C .

Downstream of the test section, the flow is diluted with atmospheric air through a vent valve to prevent further combustion in the vacuum system and in the dump tank (see Fig. 1). The $1200\ \text{ft}^3$ dump tank is pumped out using an Allis-Chalmers 1300 cfm rotary vane vacuum pump. The test section static pressure ranges from 40 torr to about 0.5 atm. The mass flow rate through the test section can be varied from below 1 g/s to 12 g/s. The test section pressure and the mass flow rate can be varied independently. This makes the experimental facility suitable for combustion studies both in high-speed, low-pressure and in low-speed, intermediate pressure flows.

The test section, made of steel, is shown in greater detail in Fig. 2. The flow enters the rectangular cross section test section through a $1/2$ inch long ceramic honeycomb flow straightener (300 holes per square inch), which also serves as a flashback arrester, and passes between two electrode blocks, as shown in Fig. 2. Each of the two 5 cm x 4 cm rectangular electrode blocks are manufactured of macor ceramic and are flush mounted in the top and bottom test section walls, as shown in Fig. 2. The copper electrode plates are placed into recesses machined in the electrode blocks. The electrodes are rounded at the edges to prevent high electric field concentration and "hot spot" formation in the plasma near the edges. The electrodes are separated from the flow by $1/16$ " thick macor ceramic plates, as shown in Fig. 2. To prevent corona discharge formation in the air pockets between the macor block, the copper electrodes, and the ceramic plates, this space is filled by a self-hardening dielectric compound (silicon rubber). The 2 mm diameter copper electrode leads are soldered to the electrode plates and insulated from the grounded test section by 10 mm outer diameter cylindrical sleeves made of macor ceramic, as shown in Fig. 2. The space between the leads and the sleeves is also filled by

the silicon rubber. Two macor ceramic inserts are also flush mounted in the side walls of the test section, as shown in Fig. 2, to prevent the discharge between the high voltage electrode and the grounded test section. Four stepped cylinder BK-7 glass windows are used to provide optical access to the discharge region through 10 mm diameter circular holes machined in the test section and in the side wall inserts, as shown in Fig. 2. The main objective of this design was to confine the discharge plasma to the area between the ceramic plates on top and bottom and between the ceramic side wall inserts, without extending to the steel walls of the test section. Striking a discharge between the high voltage electrode and a test section wall would result in arc filament and hot spot formation in the plasma. Two additional rectangular windows, also made of BK-7 glass, are located approximately 1 cm downstream of the discharge region (see Fig. 2). Finally, static pressure / flow sampling port is located at the end of the test section, as shown in Fig. 2.

The electrode blocks shown in Fig. 2 are connected to a Chemical Physics Technologies custom designed high-voltage (up to 20 kV), short pulse duration (~20-30 nsec), high repetition rate (up to 50 kHz) pulsed plasma generator. In the present experiments, the top electrode is connected to the high voltage output of the pulser, and the bottom electrode is grounded. During the pulser operation, current and voltage in the pulsed discharge are measured using a Tektronix P6015A high voltage probe and a low-capacitance resistive current probe. The current and voltage waveforms are analyzed by a 1 GHz LeCroy WavePro 7100A digital oscilloscope. The use of this pulsed power supply to provide volume flow ionization for MHD flow control and for singlet delta oxygen generation is discussed in our recent publications [16-19]. In the present work, the pulser is used to sustain a repetitively pulsed, low-temperature, uniform plasma in hydrocarbon-air flows. Images of the air plasma generated by the repetitively pulsed discharge, taken using an ICCD camera with a short exposure time (20 to 300 nsec) demonstrated that the plasma is indeed very uniform, without “hot spots” generated in the discharge [13].

Optical diagnostics used in the present work includes visible emission spectroscopy and Fourier transform infrared (FTIR) absorption spectroscopy. For the visible emission spectroscopy measurements, we used an Optical Multichannel Analyzer (OMA) with a Princeton Instruments intensified CCD array camera and a Spectra Physics 0.5 m monochromator with a 1200 g/mm grating. The emission spectra of the plasma were taken through the downstream circular window, while emission spectra of the flame were taken through the rectangular window downstream of the discharge region (see Fig. 2). The FTIR absorption spectra of the combustion products were taken with a Biorad 175C dynamic alignment FTIR spectrometer with liquid nitrogen cooled InSb detector spectrometer. For this, the flow was sampled through the static pressure / flow sampling port at the downstream end of the test section (see Fig. 2) into a 17.5 cm long cylindrical glass absorption cell with two CaF₂ windows placed into an absorption compartment of the FT spectrometer (see Fig. 1). Before sampling the flow, the absorption cell and the supply lines are evacuated using a small vacuum pump. Then the sample is drawn off until the absorption cell and the test section pressures equilibrate, after which the absorption cell shut-off valve is closed (see Fig. 1). The absorption spectra are recorded after the sample temperature reached room temperature. Basically, a small flow sample quickly cools off on its way to the absorption cell. The absorption spectra are measured at a resolution of 0.5 cm⁻¹ using an internal source (globar) of the FT spectrometer. All measurements discussed in the present paper have been done using dry air - fuel mixtures.

3. Results and Discussion

To determine the fuel vapor mole fraction in the air-fuel flow sample, with and without the plasma, we have done the following calibration procedure. The FTIR spectrometer absorption cell was filled with air and methanol vapor, with the vapor fraction in the mixture determined by measuring the cell pressure before and after adding methanol. The cell pressure was measured a few minutes after adding methanol to allow for its full evaporation and temperature equilibration. After that, the cell pressure was reduced to 20 torr by pumping the mixture out, and the absorption spectrum was taken. The methanol vapor calibration curve, plotted in Fig. 3, shows the dependence of the integrated methanol band absorption (at 2750-3100 cm^{-1}) vs. its mole fraction in the mixture. In the present experiments, this calibration curve was used to infer the methanol vapor mole fraction in the flow from the FTIR absorption spectra. The absolute uncertainty of the methanol mole fraction inference using the calibration curve shown in Fig. 3 is approximately $\pm 1\%$ mole fraction ($\pm 8\%$ relative uncertainty at stoichiometric conditions). A similar calibration curve was also obtained for ethanol.

In the present experiments, we first analyzed the effect of fuel and air flow preheating on the fuel evaporation in the test section (without plasma). These measurements have been done at the baseline conditions, in methanol-air flow at $P=90$ torr, mass flow rate $\dot{m}=1$ g/sec, and equivalence ratio $\Phi=1.2$ (15% methanol mole fraction in the flow). First, we varied the fuel preheating temperature while keeping the air flow temperature the same, $T_{\text{air}}=60^{\circ}\text{C}$. The results, plotted in Fig. 4, show that the amount of fuel vapor rather weakly depends on the fuel preheating temperature, and nearly all injected fuel is evaporated. At $T_{\text{fuel}}=20\text{-}30^{\circ}\text{C}$, the data become less reproducible, and in some runs the fuel vapor mole fraction is as low as 8-10%, while at $T_{\text{fuel}}=40\text{-}70^{\circ}\text{C}$ it remains steady at 14-15%, indicating nearly complete evaporation for $\Phi=1.2$ (see Fig. 4). Basically, Figure 4 suggests that fuel preheating does not significantly affect its evaporation in a preheated air flow.

Second, the air flow temperature was varied, while the fuel preheating temperature was kept the same, $T_{\text{fuel}}=60^{\circ}\text{C}$. These measurements showed a strong dependence of the amount of fuel vapor on the air flow temperature, as shown in Fig. 5. In this case, it is apparent that preheating the air flow is critical for accelerating fuel evaporation. Note that in this case additional fuel evaporation may also occur on the walls of the test section, whose temperature is close to the temperature of the steady-state flow of preheated air. Summarizing, the results of Figs. 4,5 show that complete fuel evaporation in the test section, without the plasma, requires operation with air flow preheated up to $T_{\text{air}}=50\text{-}60^{\circ}\text{C}$.

Figure 6 shows typical voltage and current pulses produced by the pulser connected to the two electrodes shown in Fig. 2, in air flow at $P=70$ torr and mass flow rate of $\dot{m}=0.8$ g/sec [5]. The pulse peak voltage and current are approximately 18 kV and 50 A, respectively, with the voltage pulse width at half maximum of about 30 nsec. At the baseline conditions, i.e. test section pressure and temperature of $P=0.1$ atm, $T=300$ K, the estimated peak reduced electric field in the plasma generated by the pulse is $E/N \sim 80 \cdot 10^{-16}$ $\text{V} \cdot \text{cm}^2$. Note that this upper bound estimate does not take into account the voltage fall across the plasma sheaths and the ceramic plates covering the electrodes. The pulse energy coupled to the flow, calculated from the voltage and current waveforms at these conditions, was 2.2 mJ. The accuracy in the pulse energy measurements and the effect of the parasitic phase shift between the measured voltage and the current signals were determined by measuring the voltage and current pulses when the pulser was connected to a capacitive load without producing breakdown. In this case, the pulse energy

calculated from the voltage and current waveforms (i.e. the uncertainty in the measured pulse energy) was approximately 0.2 mJ. Our previous experiments on gaseous fuel ignition [5] showed that pulse energies measured in air as well as in stoichiometric ethylene-air and methane-air mixtures, at flow rates of $\dot{m}=0.8-1.8$ g/sec and pressures of $P=70-100$ torr were similar, in the range between 1.7 mJ and 2.3 mJ.

Figure 6 also shows several voltage pulses generated at the pulse repetition rate of $\nu=40$ kHz, at the same flow conditions. From Fig. 6, it can be seen that at this pulse repetition rate the voltage duty cycle is extremely low, ~ 30 nsec / 25 μ sec $\sim 1/1000$. The high reduced electric field during the pulses makes possible efficient ionization and dissociation of molecular species by electron impact, the rates of which have strong exponential dependence on E/N [15]. On the other hand, the short pulse duration and the low duty cycle greatly improve the plasma stability. Basically, the pulse duration, ~ 30 nsec, is much shorter than the characteristic time for the ionization instability development, $\sim 10^{-3}-10^{-4}$ sec [15].

To prevent significant heating of the pulsed electrode blocks, in the present experiment the pulser run time was limited to 2-3 seconds. This time was sufficient to take visible emission spectra of the plasma and to draw a sample of the flow into the absorption cell of the FTIR. The experiments have been conducted using methanol and ethanol fuels, at test section pressures of $P=70-90$ torr, mass flow rates of $\dot{m}=1.0-2.5$ g/sec, and pulse repetition rates of $\nu=50$ kHz. As in our previous experiments [5,6], in the entire range of experimental conditions, the repetitively pulsed plasma appeared diffuse and stable. At the conditions when ignition was achieved in the test section, a flame originated in the plasma and extended downstream through the test section, visible through the rectangular optical access window (see Fig. 2).

Visible emission spectra of the plasma (partially rotationally resolved $0 \rightarrow 2$ band of the $N_2(C^3\Pi_u \rightarrow B^3\Pi_g)$ band system) have been used to infer the flow rotational temperature. For this, synthetic spectrum has been used, with the accurate nitrogen molecular constants [20], rotational like intensities [21], and the experimentally measured slit function of the spectrometer. Figure 7 shows the experimental and the synthetic $N_2(C^3\Pi_u \rightarrow B^3\Pi_g)$ emission spectra in air and in $\Phi=1.2$ methanol-air mixture, at $P=90$ torr, mass flow rate of $\dot{m}=1.0$ g/sec, $\nu=50$ kHz, and $T_{air}=T_{fuel}=60^0$ C, when ignition was achieved and flame was generated downstream of the plasma. In these two flows, the inferred rotational temperatures in the plasma are $T=240 \pm 50^0$ C and $T=480 \pm 50^0$ C, respectively.

Calibration of the spectroscopic temperature measurements has been done by comparing the synthetic and the experimental $N_2(C^3\Pi_u \rightarrow B^3\Pi_g)$ emission spectra measured in air preheated by an in-line flow heater up to $T=20-180^0$ C, at $P=70$ torr and $\dot{m}=1.0$ g/sec [5]. During the calibration, the pulse repetition rate and time-averaged discharge power were low, $\nu=5$ kHz and 2.3 mJ \cdot 5 kHz ≈ 12 W, respectively. At these conditions, the estimated flow temperature rise in the plasma is also small, $\sim 25^0$ C. Figure 8 compares plasma temperatures inferred from the nitrogen emission spectra with thermocouple measurements in the absence of the plasma, at the same location. It can be seen that the agreement between the two temperatures is very good, within the uncertainty of the temperature inference, ± 25 K. This demonstrates applicability and accuracy of this temperature measurement method at the present conditions. Note that the temperature has been measured in the discharge section (see Fig. 2), not in the flame region downstream, since $N_2(C^3\Pi_u \rightarrow B^3\Pi_g)$ emission in that region becomes very weak.

In ethanol-air flows at $P=70$ torr, $u=16$ m/sec, $\Phi=0.8-1.2$, and $T_{air}=T_{fuel}=60^0$ C, ignition was achieved but combustion was unstable, with intermittent flame clearly visible in the test section. Visual inspection of the injection nozzle spray pattern at these conditions, $\dot{m}_{fuel}=0.08-$

0.12 g/sec, showed it to be quite poor (large droplets, small spray angle). We believe that inadequate fuel injector performance at the low fuel mass flow rate is the main reason for unstable combustion at these conditions. In a methanol-air flow at the baseline conditions, at $P=90$ torr, $u=13$ m/sec, $\Phi=1.2$, and $T_{\text{air}}=T_{\text{fuel}}=60^{\circ}$ C, at a higher fuel mass flow rate of $\dot{m}_{\text{fuel}}=0.16$ g/sec, ignition was achieved and stable combustion was maintained. At this fuel flow rate, which is still below the minimum design flow rate of $\dot{m}_{\text{fuel}}=0.5$ g/sec, the injector spray pattern was noticeably better. Clearly, fuel atomization, which is critical for rapid evaporation and mixing, requires operation at significantly higher fuel and air flow rates, $\dot{m}_{\text{air}}\sim 3$ g/sec.

Figure 9 shows FT absorption spectra of the methanol-air flow sampled downstream of the discharge at these conditions, with and without the plasma. Methanol vapor absorption bands at $2750\text{-}3100\text{ cm}^{-1}$ and $3650\text{-}3750\text{ cm}^{-1}$ can be clearly seen. At these conditions, turning on the repetitively pulsed discharge resulted in flow ignition, with a flame extending through the test section. From Fig. 9, it can be seen that the use of the repetitively pulsed plasma results in a significant reduction of ethanol vapor absorption (almost by a factor of 4) and an increase in concentrations of CO, CO₂, and H₂O in the flow. As in our previous experiments on gaseous fuel ignition [4-6], oxidation of methanol does not result in its conversion to other hydrocarbons, such as methane, ethylene, or acetylene.

Figures 10 and 11 show the effect of the flow velocity in the test section on the temperature in the plasma and on the reacted fuel fraction. These measurements have been done in methanol-air flows at $\Phi=1.2$, at $P=90$ torr, $\dot{m}=1.0\text{-}2.5$ g/sec, $\nu=50$ kHz, and $T_{\text{air}}=T_{\text{fuel}}=60^{\circ}$ C. Figure 10 also shows the results of flow temperature measurements in air plasma (without fuel) at the same flow conditions, $T=130\text{-}240^{\circ}$ C. It can be seen that while both the air flow temperature and the fuel-air mixture temperature decrease with the flow velocity as it increased from $u=13$ m/sec to $u=32$ m/sec ($\dot{m}=1.0\text{-}2.5$ g/sec), the temperature of the air-fuel mixture remains significantly higher in the entire flow velocity range, by $\Delta T\sim 250^{\circ}$ C.

From Fig. 11, it can be seen that the reacted fuel fraction also decreases with the flow velocity. Unlike the results of the plasma temperature measurements, which are reproduced very well (see Fig. 10), the run-to-run reproducibility of the reacted fuel fraction measurements is not as good. At the baseline conditions (at the flow velocity of $u=13$ m/sec), the oxidized fuel fraction varies from 45% to 75% (see Fig. 11). This is most likely due to poor spray characteristics and poor mixing of the fuel injected into the air flow at the low flow rate, $\dot{m}_{\text{fuel}}=0.16\text{-}0.32$ g/sec. However, it is obvious from Fig. 11 that the reacted fuel fraction rapidly decreases with the flow velocity, down to less than 10% at $u=26$ m/sec. The flame in the test section was detected only at fairly low flow velocities, $u=13$ m/sec and 16 m/sec.

The plasma temperature rise detected in methanol-air flows compared to air flows, $\Delta T\sim 250^{\circ}$ C, is nearly independent of the flow velocity and the reacted fuel fraction (see Fig. 10), and is detected even when only a few per cent of the fuel is oxidized (see Fig. 11). Note that the discharge power in air and in air-fuel mixtures remains approximately the same (~ 100 W), and is insufficient to explain such a significant temperature rise. At $\dot{m}=1.0$ g/sec, if the entire discharge power would instantly thermalize, the flow temperature rise would be only $\sim 100^{\circ}$ C from the initial value of $T_{\text{air}}=60^{\circ}$ C, which is consistent with the air flow temperature at these conditions, $T=240^{\circ}$ C. Therefore the temperature rise after fuel injection must originate from reactions of species generated in the air plasma with fuel.

Recent measurements of O atom number density generated by a single pulse discharge in air at similar conditions, $P=60$ torr, and using an identical pulsed power supply [13] showed that it to be $n_{\text{O}}\sim 10^{14}\text{ cm}^{-3}$. At these conditions, the O atom concentration remains nearly steady

(within a factor of 2) over approximately 2 msec [13], which is close to the flow residence time in the discharge in the present experiments, 1-2 msec. Over 2 milliseconds, the flow in the discharge section is excited by approximately 100 discharge pulses, at the pulse repetition rate of $\nu=50$ kHz. Therefore, the upper bound estimate of O atom number density accumulated in the flow at these conditions is approximately $n_{\text{O}}\approx 10^{16}$ cm⁻³ (mole fraction of 0.5%). Experiments [13] also demonstrated that adding methane to air (at the equivalence ratio of $\Phi=0.5$) sharply reduces the O atom concentration, to $n_{\text{O}}\approx 10^{13}$ cm⁻³ over 2 msec, due to either accelerated O atom recombination with methane as a third collision partner or plasma chemical reactions of methane with O atoms.

Rapid recombination of 0.5% fraction of O atoms in the presence of hydrocarbons would result in flow heating by only $\Delta T\sim 40\text{-}50^{\circ}$ C, which does not explain the detected temperature rise of $\Delta T\sim 250^{\circ}$ C. Also, flow heating due to vibrational energy storage in nitrogen molecules, with subsequent rapid relaxation in presence of hydrocarbons appears very unlikely. Indeed, plasma temperature measurements in room air flows, at the conditions of Fig. 10 gave essentially the same results. If accelerated vibrational relaxation were indeed the source of the temperature rise in hydrocarbon-air flows, the temperature in a room air flow would also be significantly higher than in a dry air flow, due to rapid vibrational relaxation of nitrogen on water vapor. This suggests that the observed flow temperature rise may be due to low-temperature chain plasma chemical reactions of O atoms with hydrocarbon fuel molecules, which may generate more heat than simple O atom recombination. Note that the measured temperature rise, plotted in Fig. 10, corresponds to plasma chemical oxidation of just 2-7% of the fuel at $\Phi=1.2$ and $\dot{m}=1\text{-}2.5$ g/sec (for the stoichiometric methanol-air mixture, heat of combustion is 3025 kJ/kg).

The results of Figs. 10, 11 are consistent with the scenario suggested in our previous work on gaseous fuel ignition [5,6], that initial fuel oxidation in the plasma occurs due to exothermic plasma chemical reactions, resulting in flow temperature rise, and that ignition occurs when temperature increase due to heat generation in the plasma chemical oxidation process becomes sufficiently high. Autoignition temperature of methanol vapor at $P=1$ atm is $T_{\text{auto}}=464^{\circ}$ C, which is close to the methanol vapor / air plasma temperatures at the conditions when ignition was achieved, $T=460\text{-}480^{\circ}$ C (at $u=13\text{-}16$ m/sec, see Fig. 10). In other words, low-temperature plasma chemical fuel conversion and the related flow heating “open the door” to ignition. Additional evidence in favor of this low-temperature plasma chemical ignition mechanism could be detected in measurements of O atom and combustion product (CO and CO₂) number densities in air and in hydrocarbon-air plasmas [13], which are currently underway. These measurements would help determining whether the plasma temperature rise after fuel is added is caused by radical recombination or plasma chemical fuel oxidation.

Since at the conditions of Figs. 10, 11, at $T_{\text{air}}=T_{\text{fuel}}=60^{\circ}$ C, nearly all fuel injected into the air flow evaporated (see Figs. 4,5), these results in fact represent ignition of methanol vapor in air. To study feasibility of ignition of liquid / vapor methanol mixtures, we first reduced the air flow temperature. Figures 12 and 13 show the reacted fuel fraction and the plasma temperature at the baseline flow conditions, $\Phi=1.2$, $P=90$ torr, $\dot{m}=1.0$ g/sec, $\nu=50$ kHz, and $T_{\text{fuel}}=60^{\circ}$ C, with the air flow temperature varied in the range of $T_{\text{air}}=20\text{-}60^{\circ}$ C. From Figure 12, it can be seen that reducing the air flow temperature from $T_{\text{air}}=60^{\circ}$ C to $T_{\text{air}}=20^{\circ}$ C causes drastic reduction in the reacted fuel fraction, from 50-60% to only 2-3%. This occurs primarily because at low air flow temperatures, fuel evaporation slows down, and the fuel vapor mole fraction in the flow decreases, to 3-10% at $T_{\text{air}}=20\text{-}30^{\circ}$ C (see Fig. 5). This reduces the vapor phase equivalence ratio (i.e. the actual fuel vapor / air ratio to the stoichiometric fuel vapor /air ratio) in the flow to

$\Phi=0.25-0.8$. Basically, only a relatively small fraction of injected fuel is evaporated at these conditions. Apparently, additional heating of the air flow in the discharge, at least up to $T=200^{\circ}\text{C}$ (see Fig. 13), remains insufficient to evaporate the remaining liquid fuel at these conditions.

Figure 13 also shows that at low air flow temperatures ($T_{\text{air}}=20-30^{\circ}\text{C}$), the plasma temperature rise after the fuel is injected decreases, $\Delta T\sim 70^{\circ}\text{C}$ at $T_{\text{air}}=20^{\circ}\text{C}$, compared to $\Delta T\sim 250^{\circ}\text{C}$ at $T_{\text{air}}=50-60^{\circ}\text{C}$, when nearly all injected fuel evaporates. This shows that the plasma temperature rise after fuel injection is proportional to the fuel vapor concentration in the plasma (compare Fig. 5 and Fig. 13). The results of Figs. 12, 13 suggest that preheating of the air flow upstream of the discharge is essential for ignition because the low-temperature plasma does not supply sufficient amount of heat to evaporate preheated liquid fuel injected into a non-preheated air flow.

Second, we reduced the fuel preheating temperature from $T_{\text{fuel}}=60^{\circ}\text{C}$ to $T_{\text{fuel}}=20^{\circ}\text{C}$, still at the baseline flow conditions. From Figure 14, it can be seen that reducing the fuel temperature did not result in significant reduction of the reacted fuel fraction. In this case, the oxidized fuel fraction varies from 30% to 60% due to run-to-run variation; however, it does not exhibit a tendency to decrease as the fuel temperature is reduced. From Fig. 15, it can also be seen that in this case the temperature rise in the plasma is essentially independent of the fuel preheating temperature. Again, comparison of Fig. 4 and Fig. 15 suggest that the temperature rise in the plasma is controlled by the fuel vapor mole fraction in the flow. Indeed, in this series of experiments nearly all fuel injected into the flow evaporates (see Fig. 4), while the plasma temperature rise, $\Delta T\sim 250^{\circ}\text{C}$, remains approximately the same (see Fig. 14). In the entire range of fuel temperatures, $T_{\text{fuel}}=20-60^{\circ}\text{C}$, the reacted fuel fraction, 30% to 60%, is consistent with the results obtained at $T_{\text{air}}=T_{\text{fuel}}=60^{\circ}\text{C}$ and $\dot{m}=1.0\text{ g/sec}$ (see Figs. 12, 14). Basically, the results of Figs. 14, 15 suggest that preheating of fuel injected into a preheated air flow may be not necessary.

4. Summary

The paper presents results of plasma assisted ignition of liquid hydrocarbon fuel flows excited by a low-temperature, transverse, repetitively pulsed discharge plasma. The experiments have been conducted with methanol and ethanol fuels injected into a flow of dry air, at pressures of $P=70-90\text{ torr}$ and flow velocities of $u=13-32\text{ m/sec}$. Experiments showed that preheating of the air fuel up to $50-60^{\circ}\text{C}$ is essential for accelerating fuel evaporation in the test section. On the other hand, fuel preheating does not significantly affect fuel evaporation rate. Uniform and diffuse nonequilibrium plasma in the test section was generated by high-voltage (16-18 kV), short pulse duration (20-30 nsec), high repetition rate ($\nu=50\text{ kHz}$) pulses. In ethanol-air flows at $P=70\text{ torr}$, $u=16\text{ m/sec}$, $\Phi=0.8-1.2$, and $T_{\text{air}}=T_{\text{fuel}}=60^{\circ}\text{C}$, ignition was achieved but combustion was unstable, due to inadequate fuel injector operation (poor spray pattern) at low fuel delivery pressures and mass flow rates, $\dot{m}_{\text{fuel}}=0.08-0.12\text{ g/sec}$. In a methanol-air flow at the baseline conditions, at $P=90\text{ torr}$, $u=13\text{ m/sec}$, $\Phi=1.2$, and $T_{\text{air}}=T_{\text{fuel}}=60^{\circ}\text{C}$ ($\dot{m}_{\text{fuel}}=0.16\text{ g/sec}$), ignition was achieved and stable combustion was maintained. At these conditions, the plasma temperatures before and after fuel injection were $T=240^{\circ}\text{C}$ and $T=480^{\circ}\text{C}$, respectively, and a significant fraction of injected fuel reacted, up to 75%. Both increasing the flow velocity, up to $u=26\text{ m/sec}$, and reducing the air flow temperature, down to $T_{\text{air}}=20^{\circ}\text{C}$, resulted in drastic reduction of reacted fuel fraction, to just a few per cent. On the other hand, decreasing the fuel

preheating temperature, down to $T_{\text{fuel}}=20^{\circ}\text{C}$, did not result in a significant change of the amount of reacted fuel, which remained in the range of 30-60%. Temperature rise in the plasma caused by fuel injection is proportional to the amount of fuel vapor present in the flow without the plasma. The experiments suggest that preheating the air flow is critical for ignition, while fuel preheating may not be necessary. Further experiments using a more efficient pulser waveform (higher pulse voltage, short pulse duration, and higher pulse repetition rate) are underway. This may help achieving ignition at higher flow velocities (and higher fuel flow rates), at which fuel injector spray characteristics, and therefore fuel atomization and mixing, greatly improve.

5. Acknowledgements

This research has been supported by the Phase II AFOSR STTR grant F49620-02-C-0054. We would like to express our sincere gratitude to Sergey Gorbato from Chemical Physics Technologies, for continuing support and collaboration, as well as for his help in setting up and operating the pulsed power supply.

6. References

1. A.Yu. Starikovskii, "Plasma Supported Combustion", Proceedings of the Combustion Institute, vol. 30, 2005, 2405-2417
2. S.M. Starikovskaya, "Plasma Assisted Ignition and Combustion", J. Phys. D: Appl. Phys., vol. 39, 2006, pp. R265-R299
3. N. Chintala, R. Meyer, A. Hicks, A. Bao, J.W. Rich, W.R. Lempert, and I.V. Adamovich, "Non-Thermal Ignition of Premixed Hydrocarbon-Air Flows by Nonequilibrium RF Plasma", Journal of Propulsion and Power, vol. 21, No. 4, 2005, pp. 583-590
4. N. Chintala, A. Bao, G. Lou, and I.V. Adamovich, "Measurements of Combustion Efficiency in Nonequilibrium RF Plasma Ignited Flows", Combustion and Flame, vol. 144, No. 4, 2006, pp. 744-756
5. A. Bao, Y.G. Utkin, S. Keshav, M. Uddi, K. Frederickson, N. Jiang, W.R. Lempert, and I.V. Adamovich, "Ignition of Gaseous and Liquid Hydrocarbon Fuels by Repetitively Pulsed, Nanosecond Pulse Duration Plasma", AIAA Paper 2006-3242, 37th AIAA Plasmadynamics and Lasers Conference, June 2006, San Francisco, CA
6. G. Lou, A. Bao, M. Nishihara, S. Keshav, Y.G. Utkin, J.W. Rich, W.R. Lempert, and I.V. Adamovich, "Ignition of Premixed Hydrocarbon-Air Flows by Repetitively Pulsed, Nanosecond Pulse Duration Plasma", Proceedings of the Combustion Institute, vol. 31, Issue 2, January 2007, pp. 3327-3334
7. S.A. Bozhenkov, S.M. Starikovskaya, and A.Yu. Starikovskii, "Nanosecond Gas Discharge Ignition of H_2 - and CH_4 -containing Mixtures", Combustion and Flame, vol. 133, 2003, pp. 133-146
8. S.M. Starikovskaia, E.N. Kukaev, A.Yu. Kuksin, M.M. Nudnova M M, and A.Yu. Starikovskii, "Analysis of the Spatial Uniformity of the Combustion of a Gaseous Mixture Initiated by a Nanosecond Discharge", Combustion and Flame, vol. 139, 2004, pp. 177-87
9. N.B. Anikin, E.I. Mintousov, S.V. Pancheshnyi, D.V. Roupasov, V.E. Sych, and A.Yu. Starikovskii, "Nonequilibrium Plasmas and its Applications for Combustion and Hypersonic Flow Control", AIAA Paper 2003-1053, 41st AIAA Aerospace Sciences Meeting and Exhibit, Reno, NV, 2003

10. E.I. Mintousov, S.V. Pancheshnyi, and A.Yu. Starikovskii, "Propane-Air Flame Control by Non-equilibrium Low-temperature Pulsed Nanosecond Barrier Discharge", AIAA Paper 2004-1013, 42nd AIAA Aerospace Sciences Meeting and Exhibit, Reno, NV, 2004
11. D. Galley, G. Pilla, D. Lacoste, S. Ducruix, and C. Laux, "Plasma-Enhanced Combustion of a Lean Premixed Air-Propane Turbulent Flame using a Nanosecond Repetitively Pulsed Plasma", AIAA Paper 2005-1193, 43rd AIAA Aerospace Sciences Meeting and Exhibit, Reno, NV, 2005
12. W. Kim, H. Do, M.G. Mungal, and M.A. Cappelli, "Investigation of NO Production and Flame Structure in Plasma Enhanced Premixed Combustion", Proceedings of the Combustion Institute, vol. 31, Issue 2, January 2007, pp. 3319-3326
13. M. Uddi, N. Jiang, K. Frederickson, J. Stricker, I.V. Adamovich, and W.R. Lempert, "Spatially and Temporally Resolved Atomic Oxygen Measurements in Short Pulse Discharges by Two Photon Laser Induced Fluorescence", AIAA Paper 2007-1357, 45th AIAA Aerospace Sciences Meeting and Exhibit, Reno, NV, 2007
14. N.B. Anikin, S.M. Starikovskaya, and A.Yu. Starikovskii, "Oxidation of Saturated Hydrocarbons under the Effect of Nanosecond Pulsed Space Discharge", J. Phys. D: Appl. Phys., vol. 39, 2006, pp. 3244-3252
15. Raizer, Yu.P., "Gas Discharge Physics", Springer-Verlag, Berlin, 1991
16. M. Nishihara, N. Jiang, J.W. Rich, W.R. Lempert, I.V. Adamovich, and S. Gogineni, "Low-Temperature Supersonic Boundary Layer Control Using Repetitively Pulsed MHD Forcing", Physics of Fluids, 2005, vol. 17, No. 10, p. 106102
17. M. Nishihara, J.W. Rich, W.R. Lempert, I.V. Adamovich, and S. Gogineni, "Low-Temperature M=3 Flow Deceleration by Lorentz Force", Physics of Fluids, vol. 18, No. 8, 2006, p. 086101
18. A. Hicks, S. Norberg, P. Shawcross, W.R. Lempert, J.W. Rich, and I.V. Adamovich, "Singlet Oxygen Generation in a High Pressure Non-Self-Sustained Electric Discharge", Journal of Physics D: Applied Physics, vol. 38, 2005, pp. 3812-3824
19. A. Hicks, Yu.G. Utkin, W.R. Lempert, J.W. Rich, and I.V. Adamovich, "Continuous Wave Operation of a Non-Self-Sustained Electric Discharge Pumped Oxygen-Iodine Laser", Applied Physics Letters, vol. 89, 2006, p. 241131
20. F. Roux, F. Michaud, and M. Vervloet, "High Resolution Fourier Spectrometry of $^{14}\text{N}_2$ Violet Emission Spectrum: Extensive Analysis of the $\text{C}^3\Pi_u\text{-B}^3\Pi_g$ System", Journal of Molecular Spectroscopy, vol. 158, 1993, pp. 270-277
21. I. Kovacs, "Rotational Structure in the Spectra of Diatomic Molecules", Elsevier, New York, 1969

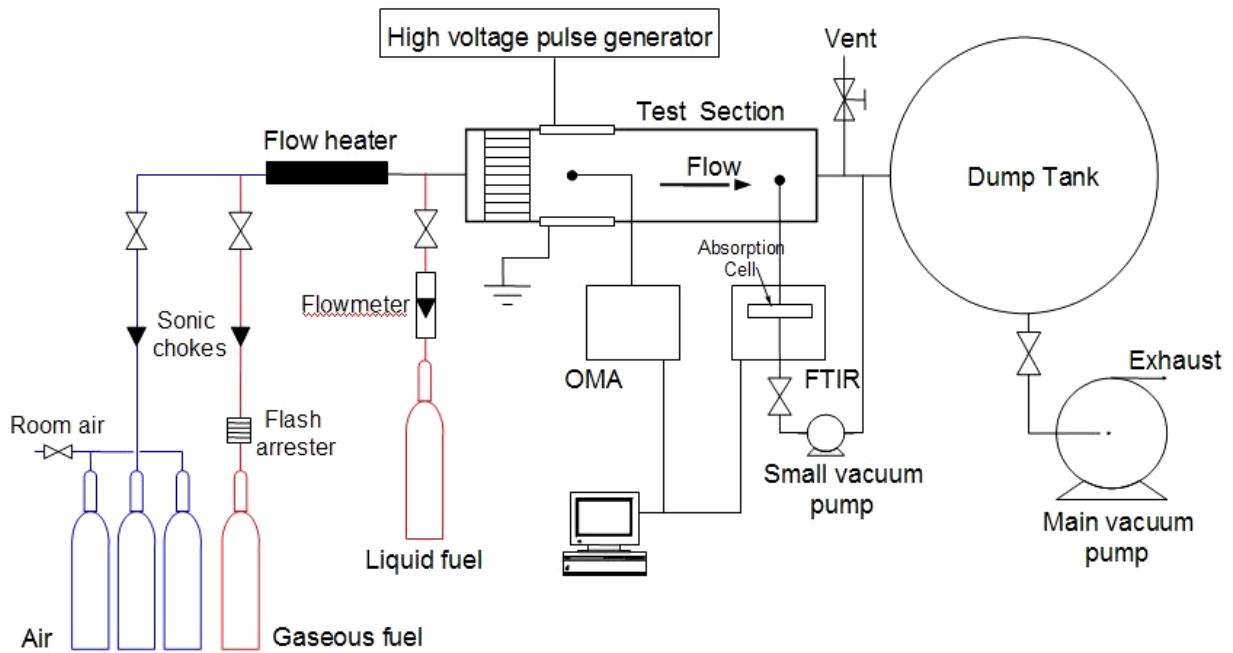


Figure 1. Schematic of the plasma combustion facility

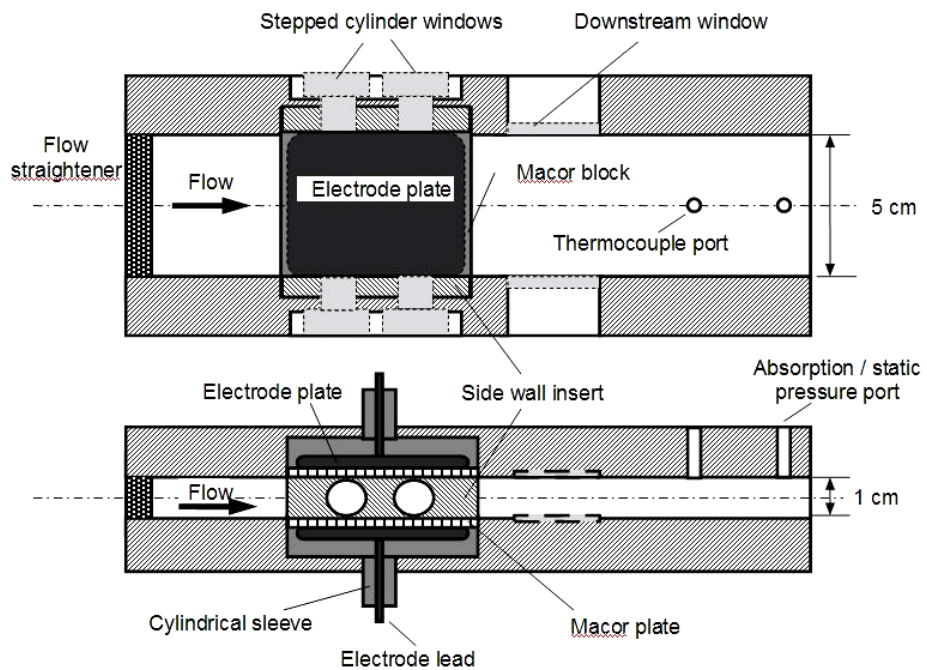


Figure 2. Schematic of the plasma assisted combustion test section

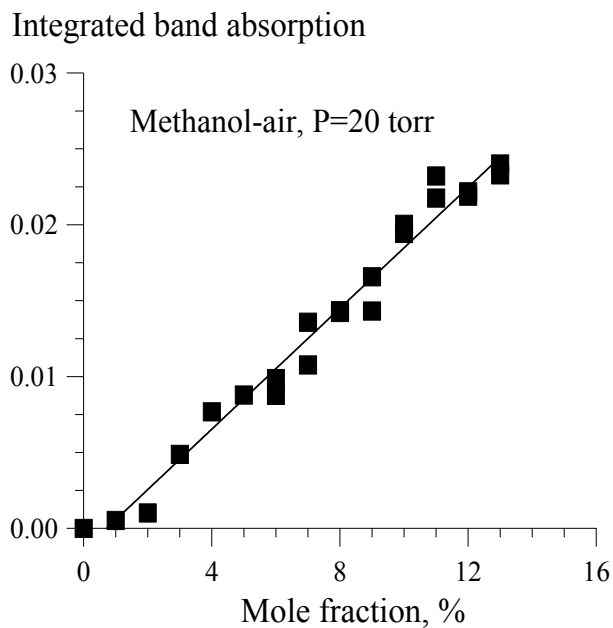


Figure 3. Methanol calibration curve.
Absorption cell pressure P=20 torr.

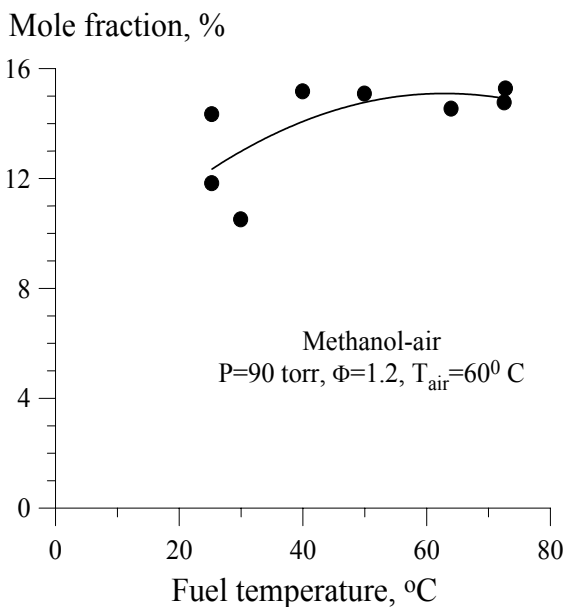


Figure 4. Fuel vapor mole fraction vs. fuel preheating temperature. Methanol-air, P=90 torr, mass flow rate $\dot{m}=1$ g/sec, equivalence ratio $\Phi=1.2$, air preheating temperature is $T_{air}=60^0$ C.

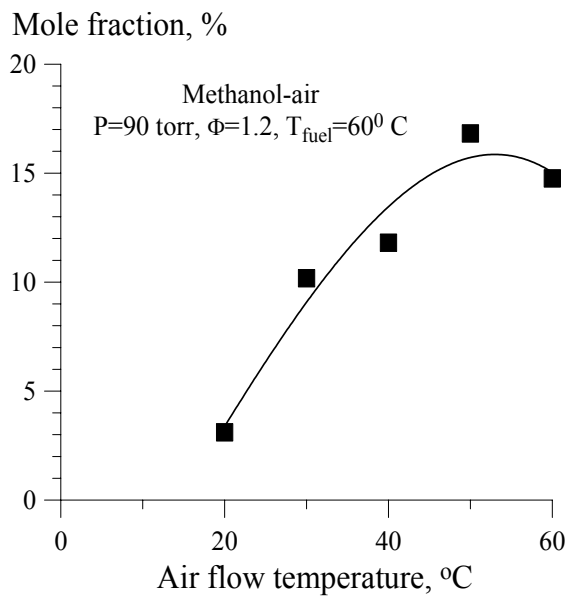


Figure 5. Fuel vapor mole fraction vs. air preheating temperature. Methanol-air, P=90 torr, $\dot{m}=1$ g/sec, $\Phi=1.2$, fuel preheating temperature $T_{air}=60^0$ C.

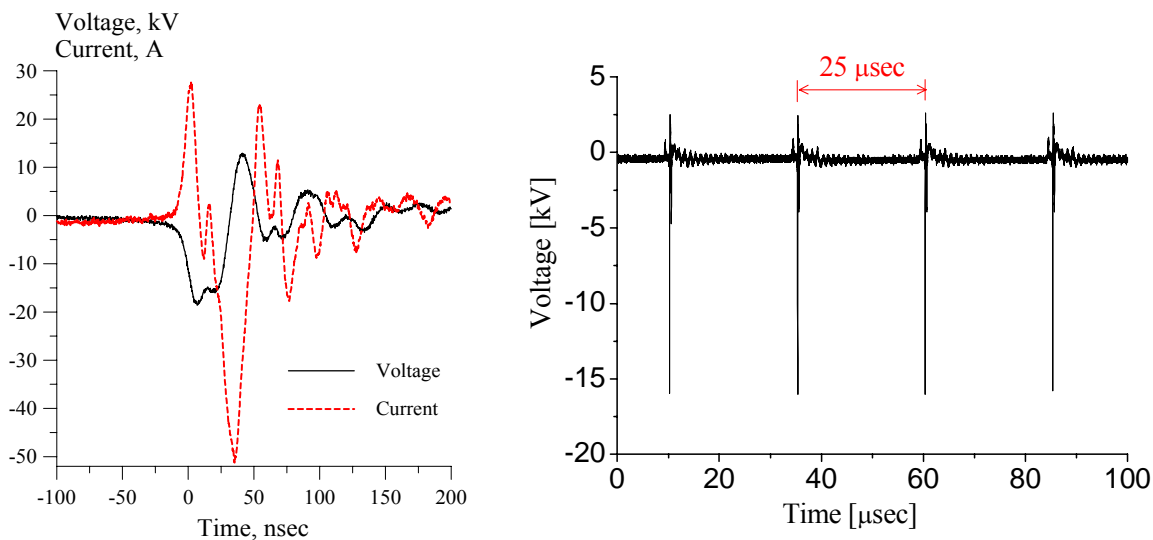


Figure 6. Typical single high voltage pulse (left) and a high voltage pulse sequence at the repetition rate of 40 kHz (right).

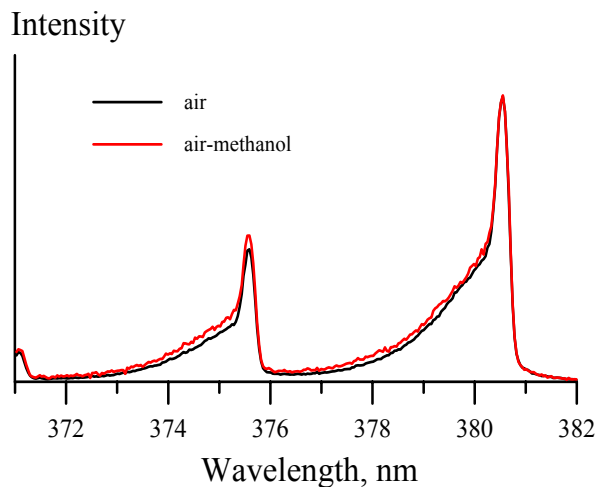


Figure 7. N_2 second positive band system spectra in air ($T=240^\circ C$) and in methanol-air mixture. ($T=480^\circ C$). $P=90$ torr, $\dot{m}=1.0$ g/sec, $\Phi=1.2$, $\nu=50$ kHz.

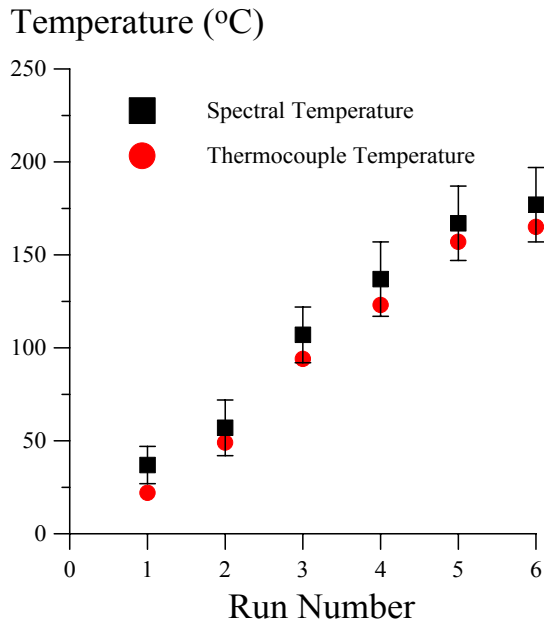


Figure 8. Comparison of preheated air flow temperatures inferred from N_2 second positive spectra with thermocouple measurements. $P=70$ torr, $\dot{m}=1.0$ g/sec, $\nu=5$ kHz, discharge power 12 W.

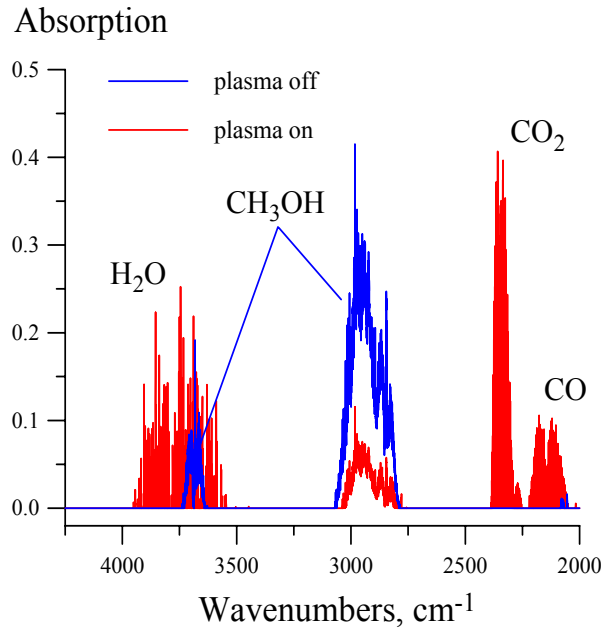


Figure 9. Typical FT absorption spectra of fuel-air flow, without and without plasma. Methanol-air, $P=90$ torr, $\dot{m}=1$ g/sec, $\Phi=1.2$, $T_{\text{air}}=60^{\circ}\text{C}$, $T_{\text{fuel}}=60^{\circ}\text{C}$.

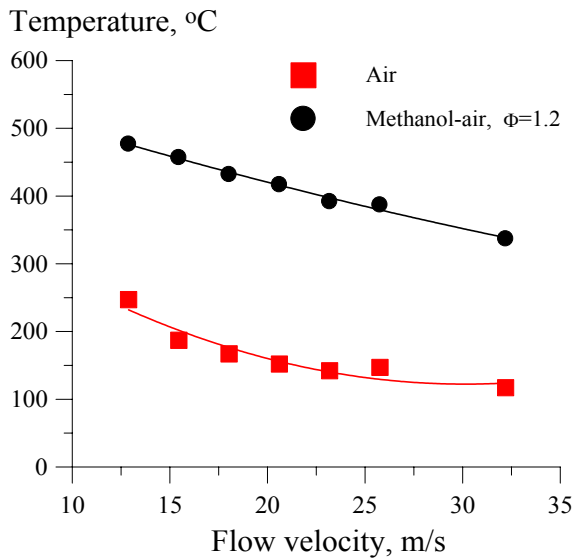


Figure 10. Flow temperature in the plasma (with and without fuel) vs. flow velocity. Methanol-air, $P=90$ torr, $\Phi=1.2$, $T_{\text{air}}=60^{\circ}\text{C}$, $T_{\text{fuel}}=60^{\circ}\text{C}$.

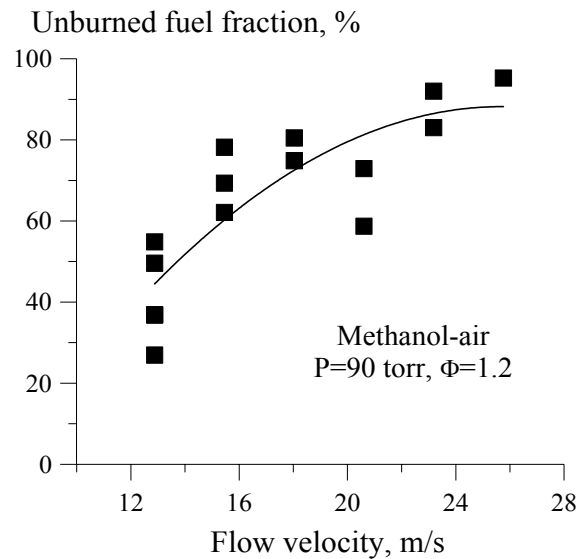


Figure 11. Unburned fuel fraction vs. flow velocity. Methanol-air, $P=90$ torr, $\Phi=1.2$, $T_{\text{air}}=60^{\circ}\text{C}$, $T_{\text{fuel}}=60^{\circ}\text{C}$.

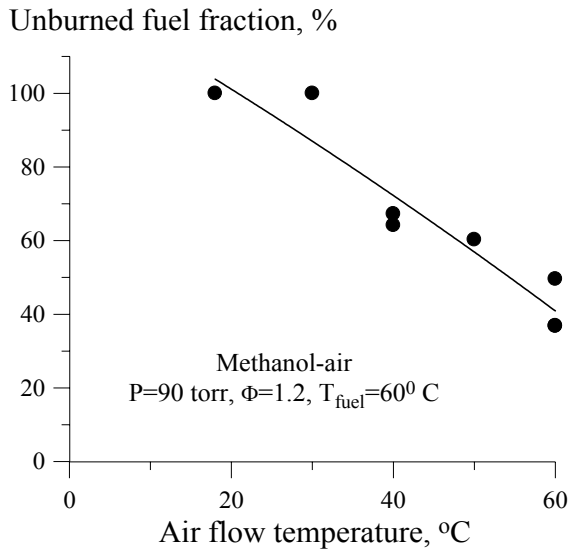


Figure 12. Unburned fuel fraction vs. air preheating temperature. Methanol-air, P=90 torr, $\dot{m}=1$ g/sec, $\Phi=1.2$, $T_{\text{fuel}}=60^{\circ}\text{C}$.

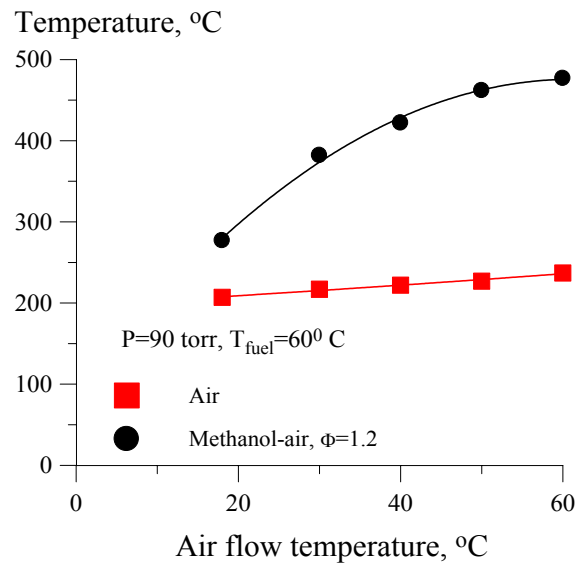


Figure 13. Flow temperature in the plasma (with and without fuel) vs. air preheating temperature. Methanol-air, P=90 torr, $\dot{m}=1$ g/sec, $\Phi=1.2$, $T_{\text{fuel}}=60^{\circ}\text{C}$.

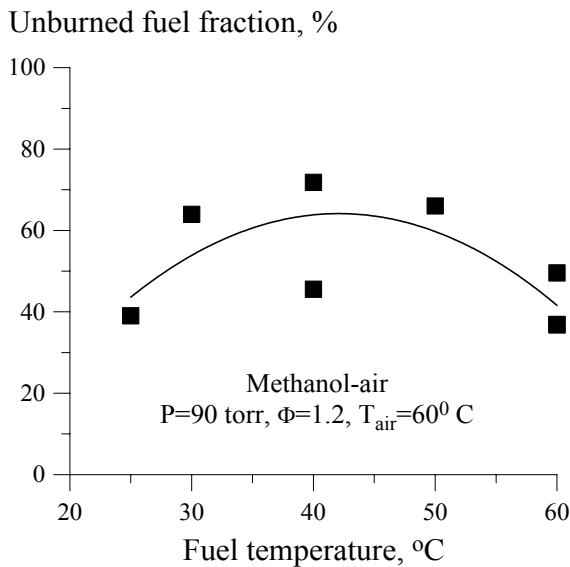


Figure 14. Unburned fuel fraction vs. fuel preheating temperature. Methanol-air, P=90 torr, $\Phi=1.2$, $T_{\text{air}}=60^{\circ}\text{C}$.

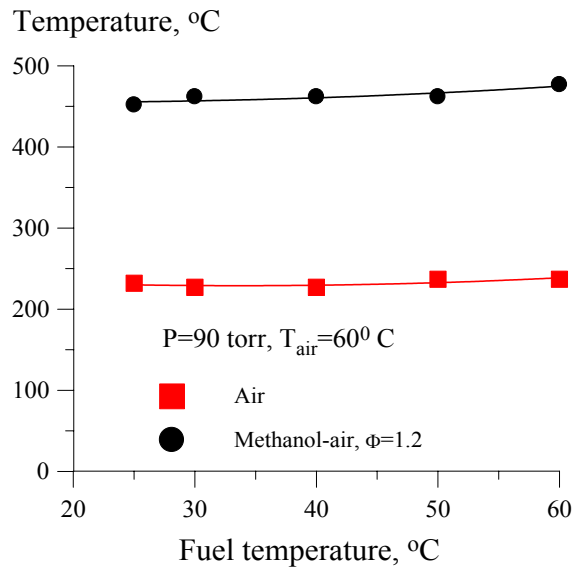


Figure 15. Flow temperature in the plasma (with and without fuel) vs. fuel preheating temperature. Methanol-air, P=90 torr, $\Phi=1.2$, $T_{\text{air}}=60^{\circ}\text{C}$.